Electrochemical Behaviour of *merdional* tris(2-pyridinethiolato)Cobalt(III) in Dimethylformamide Solution

Jung-Kyoon Chon*, Hee K. Chae*, Yongtae Kim, Yongbok Go, and Ok-Sang Jung †

Department of Chemistry, Hankuk University of Foreign Studies, Yongin, Kyungki 449-791, Korea
†Inorganic Chemistry Laboratory, Korea Institute of Science and Technology, Seoul 136-791, Korea
Received January 8, 1997

Electrochemical behavior of *mer*- tris(2-pyridinethiolato)cobalt(III) in dimethylformamide was studied on a platinum electrode by means of cyclic voltammetry, chronoamperometry, and chronocoulometry. It was found that the neutral complex molecule was electroactive between the potential region of 1.0 and − 1.2 V *vs.* a nonaqueous Ag/Ag^+ electrode. The Co(III) complex was reversibly reduced to Co(II) species by one-electron transfer at about − 1.1 V, followed by an irreversible dissociation reaction. However, the oxidation process at around 0.8 V, was responsible for an irreversible two-electron transfer that occurred at a ligand site.

Introduction

It is well known that the cobalt(III) ion forms very stable octahedral complexes with a variety of ligands containing sulfur and nitrogen donor atoms due to the high nucleophilicity of the thiolato sulfur atom.[1-5] The electrochemical behaviour of the cobalt(III) complexes has recently attracted considerable attention[4,6] because the cobalt (III) compounds exhibit the good relationship between redox potentials and ligand field energies of them. To investigate such relationship, Okuno *et al.* reported the data on both the reduction of Co(III) to Co(II) and the oxidation potentials of Co(III) to Co(IV) by RDE (rotating disk electrode) measurements.[6] However, the oxidation of Co(III) to Co(IV) was not confirmed. On the other hand, the issue whether a given electron transfer occurs at a metal or ligand site is on the rise.[7]

Studies[4,5] of tris(2-pyridinethiolato)cobalt(III), [Co(III)$(Spy)_3$], a typical 4-membered chelate on S,N-coordination, were reported to give, for the most part, its synthetic, structural, and stereochemical data. The complex [Co(III)$(Spy)_3$] has been prepared by the reaction $[Co(acac)_3]$[4] or [CoO(OH)][5] with 2-pyridinethiol [HSpy], or $[Co(H_2O)_6]Cl_2$ with $[Zn_4O(Spy)_6]$[4], and has been assigned a meridional geometry by X-ray diffractometry and NMR spectrometry. However, any electrochemical data of the complex, except the redox potential, such as reaction mechanism and kinetic data have not been found.

In this study cyclic voltammetry, chronoamperometry, and chronocoulometry of an electrochemical reaction of Co(III)$(Spy)_3$ on a platinum electrode in dimethylformamide solution were performed in order to elucidate its reaction mechanism and kinetic parameters.

Experimental

Synthesis of [Co(III)$(Spy)_3$]. Tris(2-pyridinethiolato) cobalt(III), [Co(III)$(Spy)_3$], was obtained quantitatively by modifying the literature method.[4] A mixture of $[Co(H_2O)_6]Cl_2$ (2.1 mmol) and 2-pyridinethiol potassium salt [KSpy] (7.4 mmol) in ethanol was placed in a mechanically stirred reaction vessel in the presence of air for 2 h. The dark brown reaction mixture was filtered and washed with distilled water. The crude complex was then recrystallized in acetonitile. The distorted octahedral crystal determined by X-ray crystallography, was confirmed to maintain the meridional geometry in both solid and DMF solution by NMR spectrometry. Our assignment is in good agreement with previous data.[4]

Electrochemical experiments. Dimethylformamide (DMF) and tetraethylammonium perchlorate (Et_4NClO_4) were used as received from Fluka, and *mer*- tris(2-pyridinethiolato)cobalt(III), *mer*- (Co(III)$(Spy)_3$) was prepared as mentioned above.

The electrochemical measurements were carried out with a microcomputer interfaced to an EG&G PAR model 273 Potentiostat/Galvanostat and a PAR model 377A Coulometric Cell System. The electrochemical cell was a three-compartment pyrex glass cell. The working Pt-electrode compartment was separated by a fine porosity glass-frit from the counter electrode. The reference electrode was a Ag/Ag^+ (0.1 M $AgNO_3$ in acetonitrile) electrode that encased in a bridge tube connected to the test solution by means of a fine porosity frit-tip near the working electrode. And all potential data given here referred to this reference, whose potential in test solution was 0.377 V against the SCE reference. The electrical conductivity was acquired on Philips model PM6303 RCL meter. All experiments were performed in nitrogen atmosphere at room temperature.

Results and Discussion

Cyclic Voltammetry. Figure 1 shows typical cyclic voltammogram of the solutions of *mer*- Co(III)$(Spy)_3$, HSpy (2-pyridinethiol), and KSpy (2-pyridinethiol potassium salt) in 0.1 M Et_4NClO_4/DMF. In the Figure 1, cyclic voltammogram of *mer*- Co(III)$(Spy)_3$ shows a reversible redox peak at around − 1.0 and an irreversible oxidation peak at about 0.7 volt, that are similar to those in literature,[6] whereas the reversible peak in other solutions containing HSpy or KSpy is absent. The irreversible oxidation peaks of Figure

This article is dedicated to Professor Woon-kie Paik of Sogang University in commemoration of his 60th birthday.

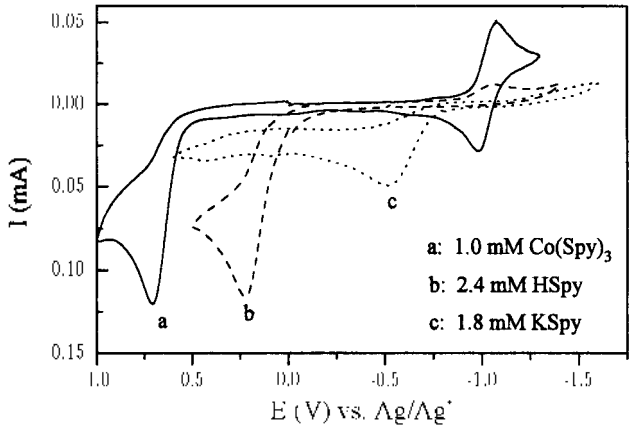

Figure 1. Cyclic voltammogram of *mer*- Co(III)(Spy)$_3$ (a), HSpy (b), and KSpy (c) in 0.10 M Et_4NClO_4 DMF at a scan rate of 100 mV/sec.

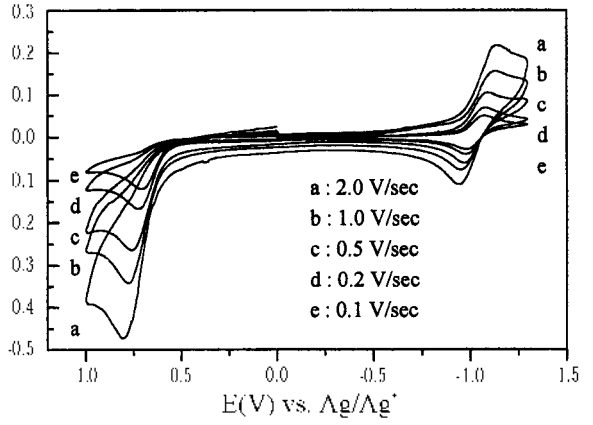

Figure 2. Cyclic voltammograms of *mer*- Co(III)(Spy)$_3$ in 0.10 M Et_4NClO_4 DMF at various scan rates in the range of 0.1 -2.0 V/sec.

1(a), (b), and (c) were observed at about 0.7, 0.2, and −0.5 volts, respectively. If the irreversible oxidation peak of Co (III)(Spy)3 corresponds to ligand [Spy] combined in the cobalt complex, more positive oxidation potential of mer-Co(III)(Spy)$_3$ than those of HSpy and KSpy indicates that the complex was more stable and the electron of ligand combined to Co(III) is more delocalized than those of HSpy and KSpy.

To present reversibility more clearly, the cyclic voltammogram of the complex at various scan rates are shown in Figure 2 and the cyclic voltammetric data are summarized in Table 1. Each peak current (i_{pc}, i_{pa}, or i_{po}) was linearly increased with increasing the square root of the scan rate (with R=0.999, refer to Figure 3). It appears that the electrochemical reduction or oxidation of the complex is a diffusion controlled reaction. In the case of redox peak under the negative potential region, the ratio (i_{pa}, i_{pc}) of the anodic to the cathodic peak-current was nearly constant to 0.9 in the range of experimental scan rates and the current function (i_{pc}, $(v)^{-1/2}$) slightly decreased with increasing the scan rate. It is speculated that the reversible electron-transfer processes are affected by a following chemical step (that is E_rC_i mechanism)[9,10] within the range of the scan rate used in this study. Under the positive potential region that only observed the oxidation peak, the current function (i_{po}, $(v)^{1/2}$) was nearly constant against the logarithmic scan rate. It seems that the oxidative process is occurring by an irreversible electron-transfer without a preceding or following chemical step.[9,10]

Table 1. Cyclic voltammetric data of 1.0 mM Co(Spy)$_3$ in 0.1 M Et_4NClO_4 DMF

Scan rate (V/sec)	$-E_{pc}$ (V)	i_{pc} (μA)	$-E_{pa}$ (V)	i_{pa} (μA)	i_{pa}/i_{pc}	$\Delta E_{p,a}$ (mV)	$i_{p,i}$ (μA)
0.02	1.074	24.1	0.990	20.5	0.85	0.676	57.1
0.06	1.074	33.2	0.980	28.4	0.86	0.698	85.2
0.1	1.076	49.9	0.982	42.8	0.86	0.708	120.3
0.2	1.082	68.7	0.979	60.6	0.88	0.726	167.7
0.5	1.097	105.5	0.966	101.3	0.96	0.762	264.2
1	1.135	155.6	0.953	138.4	0.88	0.780	342.3
2	1.140	217.5	0.942	194.7	0.90	0.900	473.5

i_{pc}: cathodic peak-current, i_{pa}: anodic peak-current, $i_{p,i}$: irreversible peak-current.

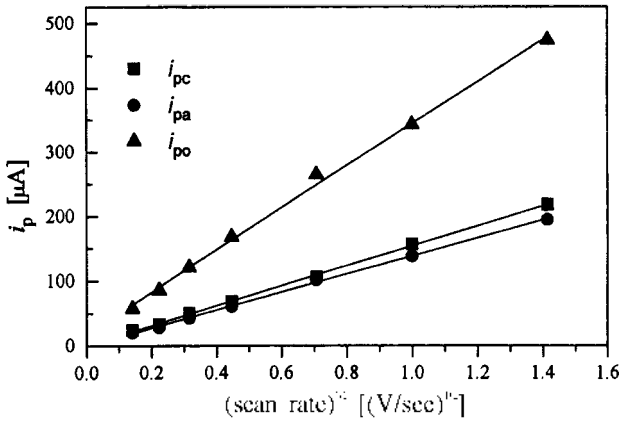

Figure 3. The relation of the peak currents to the square root of scan rate.

The irreversible anodic peak-current (i_{pa}) was about two times as much as the reversible cathodic one that was measured at each scan rate within the experimental error. Therefore, if the reversible process was one electron-transfer, the irreversible oxidative reaction maybe lose two electrons per a complex molecule. According to the Eq. (1) and (2):

$$\alpha_c = [2.3\,RT/(2\,nF)]\,[\,dE_p/d\log v\,]^{-1} \quad (1)$$

$$\alpha_a = [1.857\,RT/(nF)]\,[\,E_p - E_{p/2}\,]^{-1} \quad (2)$$

by Klinger and Kochi[16] that originally derived by Nicholson and Shain,[7] the apparent electron-transfer coefficients for reversible cathodic (α_c) and anodic (α_a), and irreversible oxidative process (α_i) were calculated 0.55(n=1), 0.45(n=1), and 0.26(n=2) from the plot of E_p *vs.* log v within the error of 5%, respectively.

Based on the argument above, we propose that an irreversible two-electron oxidation Eq. (3), a reversible one-electron redox reaction Eq. (4) and a chemical step Eq. (5) are occurring in sequence (Refer to reaction mechanism section).

$$[Co^{III}(spy)_3] + nDMF \xrightarrow[E_{ir}]{k_0} [Co^{II}(Spy)(DMF)_n]^{2+} + (Spy)_2 - 2e^- \quad (3)$$

$$[Co^{III}(Spy)_2]^- + e^- \underset{E^0}{\overset{k_s}{\rightleftharpoons}} [Co^{II}(Spy)_2]^- \quad (4)$$

$$[Co^{II}(Spy)_2]^- + H_2O \xrightarrow{k} [Co^{II}(Spy)_2]^+ + HSpy + OH^- \quad (5)$$

The linearity of Figure 3 (dependence of the peak current on the square root of the scan rate) suggests a semi-infinite diffusion response. The diffusion coefficient of depolarizer, D_{ox}, from the cyclic voltammogram (D_{ox}=5.2 x 10^{-6} cm^2/sec), was obtained from a straight line of ipc using the Randles-Sevcik equation which indicates the reversible electron-transfer:[11]

$$i_p = 0.446(nF)^{3/2}AD_{ox}^{1/2}Cv^{1/2}(RT)^{-1/2} \quad (6)$$

where n is the number of electrons passed, F is the Faraday constant, A is the electrode area, D_{ox} is the diffusion coefficient, C is the concentration of the electroactive species, v is the sweep rate, R is the gas constant, and T is the absolute temperature.

Potential Step Chronoamperometry. Figure 4 illustrates Cottrell plot, for time up to 2.0 s. This plot is linear and exhibit a nearly zero current intercept, which is consistent with a semidiffusion response. A diffusion coefficient was estimated from this plot using the Cottrell equation and is identified as D_{ps}, where ps signifies potential step (D_{ps}=7.8 x 10^{-6} cm^2/sec):

$$i(t) = nFAD_{ps}^{1/2}C^*(\pi t)^{-1/2} \quad (7)$$

Migration enhancement on the diffusional response may be diagnosed by a non-zero intercept in the Cottrell plot,[12] but this feature was not observed in this investigation. D_{ps} is larger than D_{cv} within the same order of magnitude. The dependence of the diffusion coefficient on the experimental technique used in its measurement is also observed by Foster and Vos.[13] It has been proposed that these differences may represent a dependence on the experimental time scale. The nature of the rate determining step is not dependent on the experimental time scale and the larger activation energy for the cyclic voltammetry reflects a greater diffusional motion limitation. It is not surprising, considering the nature of diffusional motion is decidely different from each other technique.

To elucidate of the rate constant for the following chemical reaction, we applied the double potential step technique, and typical current time curves were obtained like as Figure 5. The dimensionless ratio of the anodic to cathodic current (i_a/i_c), which measured at the time t and (t- τ), respectively, was simplified to Eq. (8) by Schwarz and Shain.[7]

$$-\frac{i_a}{i_c} = \phi[k_\tau(t-\tau)/\tau] - \sqrt{\frac{(t-\tau)/\tau}{1+(t-\tau)/\tau}} \quad (8)$$

$$\phi = e^{-k\tau/2}I_0(k\tau/2) + 2e^{-k\tau/2}e^{-k(t-\tau)} \times \sum_{n=1}^{\infty} I_n(k\tau/2)\frac{\int_0^{k(t-\tau)}\cdots\int_0^{\lambda_2}\lambda_1^n e^{\lambda_1}d\lambda_1\cdots d\lambda_n}{[k(t-\tau)]^n}$$

where $I_n(k\tau/2)$ represents the modified Bessel functions and k is the rate constant of the following chemical step. When the time ratio, $(t-\tau)/\tau$, is 1.0, the working curve ($-i_a/i_c$ vs. k) is shown in Figure 6. From the observed current ratio, ($-i_a/i_c$ =0.18 ± 0.01), the rate constant, k, was calculated at 0.13 ± 0.01 sec^{-1}.

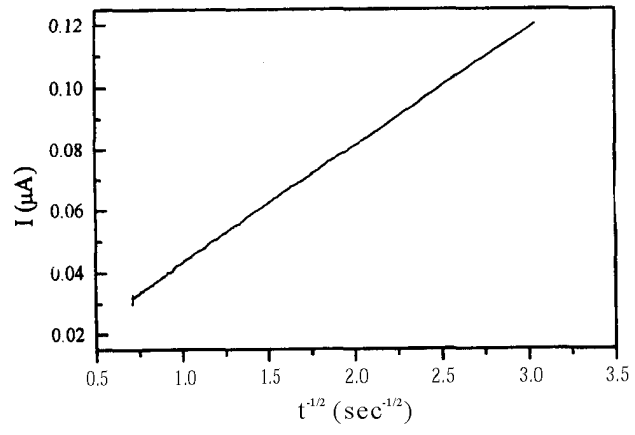

Figure 4. Typical Cottrell plot for the reduction at − 1.2V.

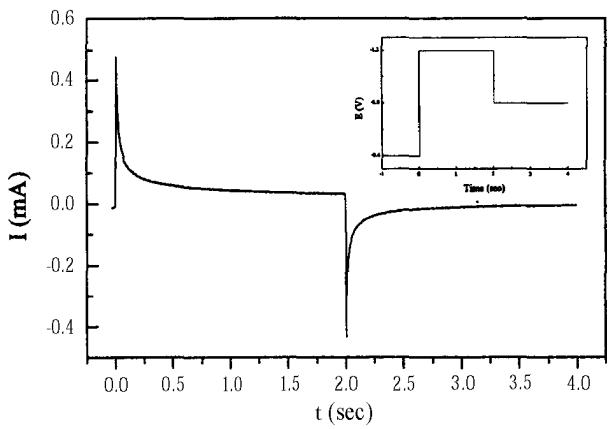

Figure 5. Typical relation of current to time for double potential step chronoamperometry.

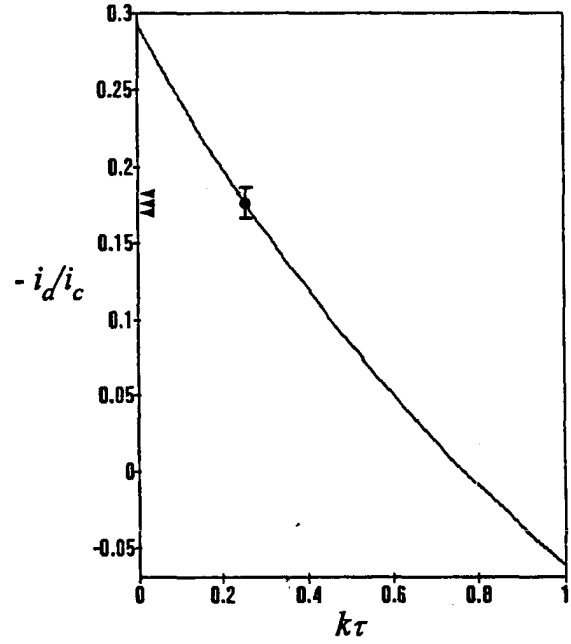

Figure 6. Comparison of experimental data with theoretical working curve of double potential step i-t transient an EC mechanism, when $(t-\tau)/\tau$ 1.0.

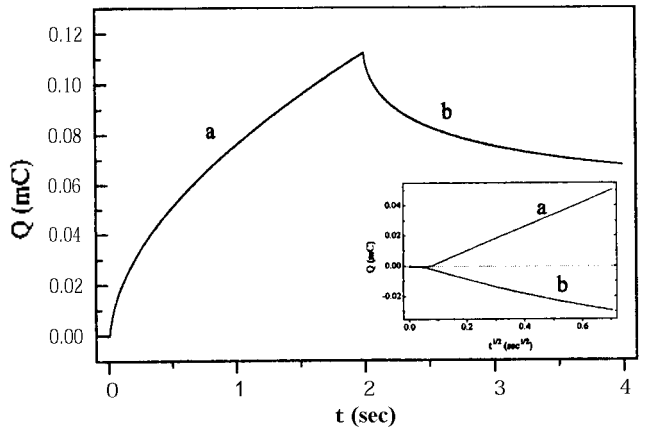

Figure 7. Typical relation of charge to time for double potential step chronocoulometry.

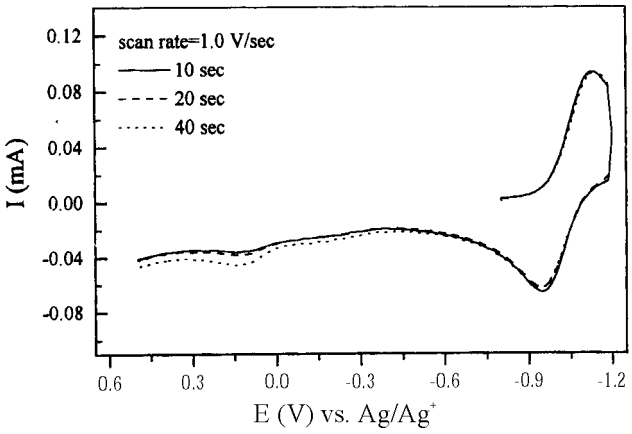

Figure 8. Voltammograms after reduction at − 1.2 V during a given period.

Potential Step Chronocoulometry. Electrochemical rate constants can be measured by using of a short-time chronoamperometric technique. The current-time transient in response to a higher overpotential step from a potential where no current flowed for the electrode reaction, even though the process is reversible, shows a linear plot of I *vs.* $t^{-1/2}$ at short time with intercept $I_{t=0}$, given by,[7]

$$I_{t=0} = nFkC^{*} \qquad (9)$$

from which the potential dependent rate constant k can be obtained. However, the advantage of chronocoulometry over chronoamperometry is that since the total charge is the sequent intergral of the current it minimizes the uncertainty due to the double layer charging process. If total charge, Q, is plotted as a function of $t^{1/2}$, the data asymptote to the straight line defined by Eq. (10)[8]

$$Q = (4nFk/\pi)C^{*}(t_{c}^{1/2}t^{1/2} - t_{c}) \qquad (10)$$

where t_c is the intercept on the x-axis. The value k is obtained from the slope and the value of t_c. Figure 7 shows a typical example of a Q-t and Q-$t^{1/2}$ plot. By using Eq. (10) and Figure 7, the rate constants (at step-potential) were obtained as k_f(− 1.2 V)=0.035, k_f(− 0.8 V)=0.055, and k_b(0.9 V)=0.021 cm/sec within the error of 5%, respectively.

The potential dependence of the rate constant in a reversible reaction (refer to Eq. (4)) is usually written as

$$k(E) = k_s \exp[(\beta nF(E - E^{\circ}))/RT], \beta = \alpha_a \text{ or } -\alpha_c \qquad (11)$$

where E is the electrode potential, is the transfer coefficient for the electrode process, n is the number of electrons transferred in the rate-determining step, and E° is the standard potential and k_s is the standard rate constant (at $E = E^{\circ}$).[10,14] In other words, for a totally irreversible process, the electron-transfer rate constant at the cyclic voltammetric peak potential, $k(E_p)$ is directly related to the sweep rate v and the diffusion coefficient D and given by Eq. (12)[9,10]

$$k(E_p) = 2.18[D\beta nFv/(RT)]^{1/2} \qquad (12)$$

By using the Eq. (11) and (12), the standard rate constants for electron transfer Eqs. (3) and (4) were obtained as k_s(irr., 0.9 V)=0.021 cm/sec and k_s(rev) 3.0 × 10^{-3} cm/sec, respectively.

Reaction Mechanism. When the complex, $Co(Spy)_2$, is dissolved in oxygen-free DMF, undissociated neutral species of $Co(Spy)_2$ will be probably dominant over the others due to the conductivity data. [The conductivity γ of 0.1 M solution of $Co(Spy)_2$, HSpy, KSpy, and $NaClO_4$ in DMF were 0.4, 1.3, 54, and 90 μ S/cm, respectively.] It has been, thus, proposed that this neutral species is electroactive at the potential range tested in this work. The reversible cyclic voltammogram in Figure 2 can be originated from the reduction of the electroactive Co(III) species, $[Co(Spy)_2]$ and the oxidation of a greater part of the Co(II) species, $[Co(Spy)_2]^{-}$ that is produced during reduction. However, a small part of the reduced species is probably dissociated to $[Co(Spy)_2]$ and (Spy^{-}). The dissociated species, (Spy^{-}) will deduct a proton from H_2O molecule that partly presents in DMF, and then produce HSpy.

According to Marcus theory,[7] the rate of electron transfer can be indicative of the site of charge transfer in a coordination compound. Owing to the chronocoulometric measurements, the heterogeneous rate constant (2.1 × 10^{-2} cm/sec) of the irreversible oxidative reaction was larger than that (3.0 − 10^{-3} cm/sec) of the reversible reduction. We conclude from this observation that the irreversible oxidation wave under the positive potential region (the left-handed side of the Figure 2) corresponds to a ligand-centered oxidation, whereas the reversible wave under the negative potential depicts a metal-centered redox reaction.

In order to confirm the reaction product, the cyclic voltammograms after electrolyzed at − 1.2 or 0.8 V during a given period were obtained and are shown in Figures 8 and 9, respectively. In Figure 8, the anodic waves appeared at about 0.15 V were increased with increasing the reduction-period at − 1.2 V, whereas the oxidation waves at around − 1.0 V were not changed. It seems that the chemical species oxidized at 0.15 V is not to be (Spy^{-}), rather to be (HSpy) (refer to Figure 1). In Figure 9, all peak currents kept nearly constant in any case. In addition, the reduction peak-currents of Figure 9 at about − 1.1 V were reduced to halves of those of Figure 8. It is speculated that the species oxidized at 0.8 V will not be electroactive in the potential region tested here and the most part of the species remains at a diffusion layer during the experimental time scale.

Based on the above argument, the following scheme is

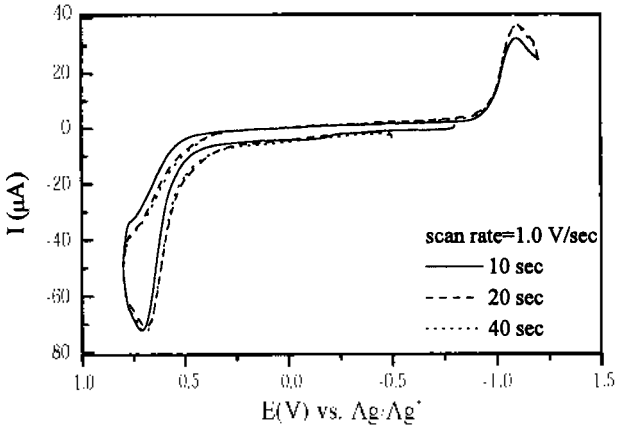

Figure 9. Voltammograms after oxidation at 0.8 V during a given period.

Table 2. Kinetic parameters for the proposed mechanism of Co (III)(Spy)$_3$

E^0 (V)	α_c	α_a	α_c	D_0 (cm^2/ sec)	k_s (cm/ sec)	k (1/sec)	E_{ir} (V)	k_0 (cm/ sec)
-1.003	0.55	0.45	0.26	7.8×10^{-7}	3.0×10^{-3}	0.13	0.460	0.021

postulated as a probable reaction mechanism of [Co(III)(Spy)$_3$] and the kinetic parameters are summarized in Table 2.

Metal-centered redox reaction

$$[Co^{III}(Spy)_3] + e^- \underset{E^0}{\overset{k_s}{\rightleftharpoons}} [Co^{II}(Spy)_3]^-$$

$$[Co^{2}(Spy)_3]^- + H_2O \text{ (in DMF)} \xrightarrow{k} [Co^{2}(Spy)_2] + HSpy^- + OH^-$$

Ligand-centered oxidation

$$[Co^{II}(Spy)_3] + n\ DMF \xrightarrow[E_{ir}]{k_0} [Co^{II}(Spy)(DMF)_{n-1}]^{+} + (Spy)_2 + 2e^-$$

Acknowledgment. This study was partially supported by Hankuk University of Foreign Studies, Center for Inorganic Materials Chemistry at Chungnam National University, and Department of Education, Basic Science Research Institute Program under contract BSRI-95-3407.

References

1. Kita, M.; Yamanari, K.; Shimura, Y. *Bull. Chem. Soc. Jpn.* **1982,** *55*, 2873.
2. Kita, M.; Yamanari, K.; Shimura, Y. *Chem. Lett.* **1983,** 141.
3. Kita, M.; Yamanari, K.; Shimura, Y. *Chem. Lett.* **1984,** 297.
4. Consable, E.; Palmer, C. *Inorg. Chim. Acta* **1990,** *176*, 57.
5. Yamanari, K.; Dogi, S.; Okusako, K.; Fujihara, T.; Fuyuhiro, A.; Kaizaki, S. *Bull. Chem. Soc. Jpn.* **1994,** *67*, 3004.
6. Okuno, M.; Kita, M.; Kashiwabara, K.; Fujita, J. *Chem. Lett.* **1989,** 1648.
7. Schultz, F. A.; Mu, X. H. *Inorg. Chem.* **1990,** *29*, 2877.
8. Lenhart, N.; Singer, H. Z. *Naturforsh, Teil B* **1975,** *30*, 284.
9. (a) Nicholson, R.; Shain, I. *Anal. Chem.* **1964,** *36*, 706. (b) Nicholson, R.; Shain, I. *Anal. Chem.* **1965,** *37*, 178. (c) Schwarz, W. M.; Shain, I. *J. Phys. Chem.* **1965,** *69*, 30.
10. Klinger, R. J.; Kochi, J. K. *J. Phys. Chem.* **1981,** *85*, 1731.
11. Bard, A. J.; Faulkner, L. R. *Electrochemical Methods;* John Wiley: New York, 1980; p 218.
12. Kelly, D. M.; Vos, J. G. *Electrochim. Acta* **1996,** *41*, 1825.
13. Foster, R. J.; Vos, J. G. *Electrochim. Acta* **1992,** *37*, 159.
14. Robinson, J. *Instrumental Methods in Electrochemistry;* Ellis Horwood: Chichester, 1985; Chap. 2.